Atmospheric Environment 292 (2023) 119414

Contents lists available at ScienceDirect

Atmospheric Environment

journal homepage: www.elsevier.com/locate/atmosenv

Spatial distribution of marine atmospheric isoprene in the Southern Hemisphere: Role of atmospheric removal capacity

Xiawei Yu [a], Yanli Zhang [b], Ruilin Jin [a], Zhangyan Chai [c], Qihou Hu [d], Juan Yu [a], Jie Xing [a], Lulu Zhang [a], Hui Kang [a], Yanxu Zhang [e,**], Xinming Wang [b,***], Zhouqing Xie [a,c,*]

[a] Institute of Polar Environment & Anhui Province Key Laboratory of Polar Environment and Global Change, Department of Environmental Science and Technology, University of Science and Technology of China, Hefei, Anhui, 230026, China
[b] State Key Laboratory of Organic Geochemistry, Guangzhou Institute of Geochemistry, Chinese Academy of Sciences, Guangzhou, 510640, China
[c] School of Life Sciences, University of Science and Technology of China, Hefei, Anhui, 230026, China
[d] Key Lab of Environmental Optics and Technology, Anhui Institute of Optics and Fine Mechanics, Chinese Academy of Sciences, Hefei, 230031, China
[e] Joint International Research Laboratory of Atmospheric and Earth System Sciences, School of Atmospheric Sciences, Nanjing University, Nanjing, 210023, China

HIGHLIGHTS

- Maine atmospheric isoprene has a negative correlation with latitude.
- Observed marine atmospheric isoprene concentration 2–3 orders of magnitude higher than the model estimated.
- Atmospheric removal capacity is an important factor for marine atmospheric isoprene in latitudes south of 60°S.

ARTICLE INFO

Keywords:
Isoprene
Spatial distribution
Influencing factors
Marine emission capacity
Atmospheric removal capacity

ABSTRACT

Isoprene is important to the formation of secondary organic aerosols and can change the atmospheric oxidation capacity in the remote marine environment. However, the influencing factors of marine atmospheric isoprene are still unclear. Here, we report observed atmospheric isoprene in ambient air along three cruises path from the Arctic Ocean to the Southern Ocean. The levels of isoprene ranged from not detected (ND) to 452 pptv, with an average value of 48 ± 81 pptv, with large variability. A negative correlation was found between isoprene and latitude ($r = -0.40$, $p < 0.01$). The spatial distributions of isoprene flux from oceanic phytoplankton by the modelled results were different from those of observed atmospheric isoprene. The observed isoprene concentration was 2–3 orders of magnitude higher than the model estimation. Environmental variables such as temperature, wind speed (WS), sea surface temperature (SST), salinity and atmospheric removal capacity can influence the distribution of isoprene. At latitudes north of 60°S, the marine emission capacity was relatively important and contributed 45.06%. Atmospheric removal capacity was the most important factor for atmospheric isoprene, contributing 55.05% to the concentration of atmospheric isoprene in latitudes south of 60°S. Low atmospheric oxidation capacity and wind speed cause high atmospheric isoprene in the Southern Ocean in summer and will eventually affect secondary organic aerosol concentrations.

1. Introduction

Isoprene is one of the dominant compounds of biogenic volatile organic compounds (BVOCs), with global continental emissions of approximately 500–750 Tg yr^{-1} (Guenther et al., 2006). Isoprene has also been suggested as a significant precursor of secondary organic aerosols (SOAs) and is important to atmospheric chemistry; it can react with ozone, hydroxyl radicals (OH) and nitrogen oxide radicals (Böge

* Corresponding author. Institute of Polar Environment & Anhui Province Key Laboratory of Polar Environment and Global Change, Department of Environmental Science and Technology, University of Science and Technology of China, Hefei, Anhui, 230026, China.
** Corresponding author.
*** Corresponding author.
E-mail addresses: zhangyx@nju.edu.cn (Y. Zhang), wangxm@gig.ac.cn (X. Wang), zqxie@ustc.edu.cn (Z. Xie).

https://doi.org/10.1016/j.atmosenv.2022.119414
Received 9 May 2022; Received in revised form 6 September 2022; Accepted 28 September 2022
Available online 5 October 2022

et al., 2006; Bates and Jacob, 2019; Claeys et al., 2004). Compared with terrestrial emissions, isoprene emissions of global oceanic (0.32–11.6 TgC yr^{-1}) is small (Conte et al., 2020; Luo and Yu, 2010). However, due to its fast reaction with OH (Wennberg et al., 2018), the atmospheric oxidation capacity could potentially be influenced by isoprene in a remote marine atmosphere (Lewis et al., 2001; Liakakou et al., 2007). Although marine isoprene emissions are far less than DMS emissions, the production of SOAs from isoprene is high (Novak and Bertram, 2020), and biogenic-origin SOAs may have an important role in cloud formation in clean background environments (Meskhidze and Nenes, 2006).

A previous field study of marine atmospheric isoprene found that marine atmospheric isoprene can be influenced by land emissions; for example, in the southern Indian Ocean, a high level of 280 parts per trillion by volume (pptv) of isoprene was observed (Yokouchi et al., 1999). In addition, temperature, light intensity and phytoplankton species may be responsible for the different spatial distributions of atmospheric isoprene. Shaw et al. (2003) studied isoprene production by phytoplankton such as *Prochlorococcus, Synechococcus* and others, the results found that the production rates of isoprene by per phytoplankton cell changed with the cellular growth phase and that the production of isoprene was increased at high light levels (100 μE $m^{-2}s^{-1}$). In addition to the biogenic source of marine isoprene, some studies have reported that abiotic processes can also produce isoprene. Photochemical reactions at the sea water−air interface are an important source of abiotic isoprene and have a potential contribution of more than 60% to organic aerosol mass in the sea-surface microlayer (SML) over the remote ocean (Brüggemann et al., 2017, 2018; Ciuraru et al., 2015). According to oceanic chlorophyll-*a* concentrations, model simulation results showed large uncertainties (Palmer and Shaw, 2005). Based on the "bottom-up" and "top-down" methods to evaluate global oceanic emissions of isoprene, the emissions were 0.32 TgC yr^{-1} and 11.6 TgC yr^{-1} of the "bottom-up" and "top-down" methods, respectively, almost 2 orders of magnitude (Luo and Yu, 2010). Marine atmospheric isoprene is influenced by the sea-air exchange flux and atmospheric oxidation (Booge et al., 2018; Wells et al., 2020). In addition, some isoprene sources might be missing in previous studies (Booge et al., 2016; Fu et al., 2019; Wells et al., 2020).

In recent years, global warming has caused a series of changes in sea surface temperature, sea ice concentration, marine ecological environment and so on (IPCC et al., 2018; 2019). Due to the potential influence of BVOC on atmospheric oxidation and climate effects (Shaw et al., 2010), more field observations are needed in the ocean, especially in the remote ocean with these changes coming. This work provides the updated levels and spatial distribution of ship-based measurements of atmospheric isoprene over a large latitude range. Combined with the simple modelled emission of isoprene sources, the potential influencing factors of marine atmospheric isoprene are discussed.

2. Methods

2.1. Field sampling

Samples were collected on the *R/V Xuelong* during the 5th China Arctic Research Expedition (CHINARE2012, from July 2012 to September 2012), 28th China Antarctic Research Expedition (CHINARE2011/2012, from November 2011 to April 2012), and 29th China Antarctic Research Expedition (CHINARE2012/2013, November 2012 to April 2013), as shown in Fig. 1. The cruises of CHINARE2012 travelled from the East China Sea to the Arctic Ocean, and CHINARE2011/2012 and CHINARE2012/2013 all travelled from the East China Sea to the Antarctic region. Cleaned and air-evacuated 2 L electropolished stainless steel canisters were used for atmospheric isoprene sample collection at the fifth fore deck of the *R/V Xuelong*, approximately 30 m above sea level (He et al., 2016). The canisters were cleaned with high-purity nitrogen gas more than five times before the sampling operation and then use a rotary vane pump (Alcatel, 2008A) to vacuum the canisters and lower the pressure in the canister to less than 3 Pa. Details of the steps were described by Hu et al. (2016) and Blake et al. (1994). Before sampling, the cover of the canister's air inlet port was taken off and kept upwind for 2–3 min. Air was blown in the fore-pipeline. Then, the valve of the canister was opened, and each air sample was collected upwind for 5 min. After the air inflow sound

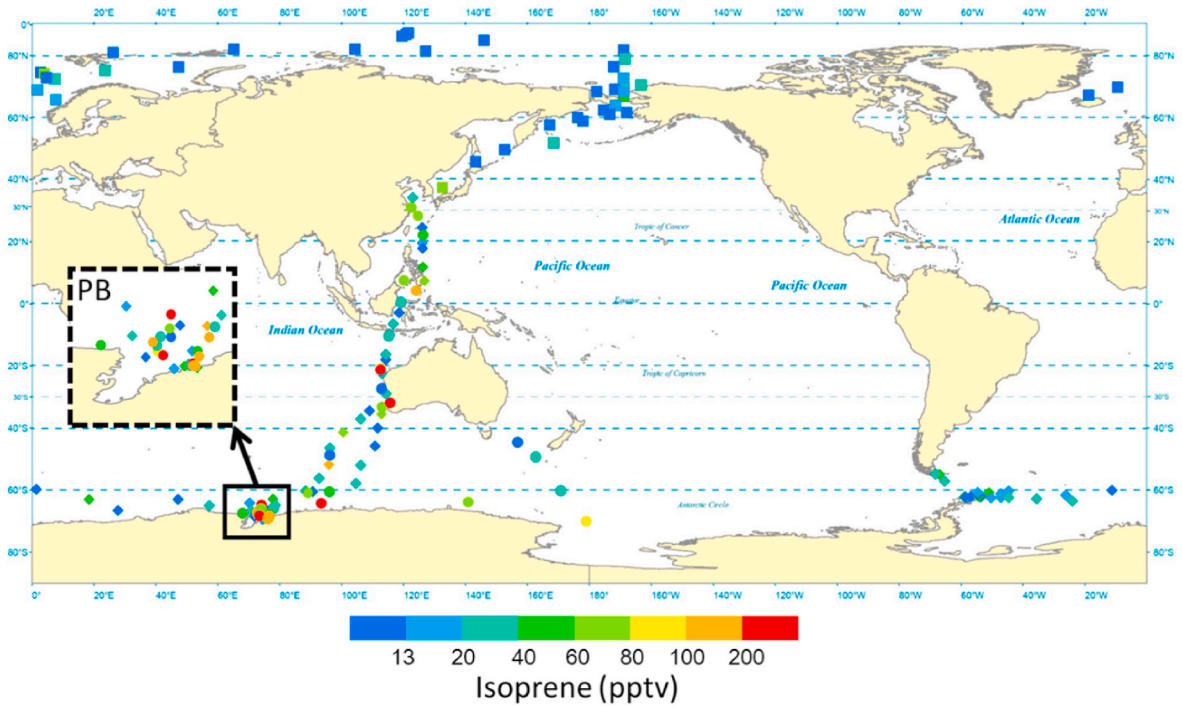

Fig. 1. Spatial distributions of isoprene over oceans. The square indicates CHINARE2012, the cycle indicates CHINARE2011/2012 and the diamond indicates CHINARE2012/2013. PB: Prydz Bay.

disappeared, it was balanced for 1 min, and then the canister valve was closed. Air samples were analysed at the Guangzhou Institute of Geochemistry, Chinese Academy of Sciences, after the campaigns finished.

2.2. Laboratory analysis and data processing

The detailed steps of laboratory analysis and quality control and assurance of the canister air samples were described by previous studies (Hu et al., 2016; Zhang et al., 2012). A preconcentrator (Entech Instruments Inc. Model 7100, California, USA) connected with an Agilent 5973 N gas chromatography-mass selective detector/flame ionization detector (GC−MSD/FID, Agilent Technologies, USA) was used. First, 500 ml air samples were enriched in a liquid-nitrogen cryogenic trap at −160 °C and then heated to 10 °C. The trapped samples were adsorbed by Tenax-TA and carried by helium into a secondary trap at −40 °C. After these steps, the target compound was then heated and transferred by helium to a third cryo-focus trap at −170 °C. Then, the temperature was rapidly raised to transfer the enriched compound into the GC−MSD/FID system for analysis. A DB-1 capillary column (60 m × 0.32 mm × 1.0 μm, Agilent Technologies, USA) was used. The GC oven temperature was initially set at −50 °C for 3 min and increased to 10 °C at 15 °C min^{-1}, then 120 °C at 5 °C min^{-1}, then 250 °C at 10 °C min^{-1} and remaining at 250 °C for 10 min. The MSD was used in selected ion monitoring (SIM) mode.

To ensure the validity of the standard curve quantification, the standard sample with a concentration of 1 ppbv was measured before analysing the samples, and the existing standard curve was used for quantification. The deviation of the quantitative result from the theoretical concentration value was less than 10%; if the deviation was greater than the range, the standard curve was recalibrated. In addition, blank tests to ensure that no target compounds were detected or were under the detection limit were undertaken. The method detection limit of isoprene was 13 pptv. For the calibration of isoprene, this information was added as supplementary information (Fig. S1).

The atmospheric isoprene data were prescreened to avoid contamination from the vessel's exhaust. CO, benzene, and toluene were used as contamination markers to filter the data, and detailed information is shown in the supplementary information.

2.3. Supporting data sources, air mass back trajectories and statistical analysis

The sea surface temperature (SST), air temperature (T), salinity and wind speed (WS) data were taken from ship-borne measurements. The formaldehyde (HCHO) was obtained from Tropospheric Emission Monitoring Internet Service (https://disc.gsfc.nasa.gov/datasets/OMHCHOd_003). To identify the influence from the continent, the HYbrid Single Particle Lagrangian Integrated Trajectory (HYSPLIT) transport and dispersion model of the NOAA Air Resources Laboratory (http://ready.arl.noaa.gov/HYSPLIT.php) was used for modelling of 2-day air mass back trajectories (BTs). Thirty-two samples were found to be influenced by the air mass passing through the continent, accounting for approximately 20% of the samples discussed in this study.

The isoprene concentration under the method detection limit was counted as 0, which may cause the average value to be lower than the actual atmospheric concentration. IBM SPSS Statistics 20 was used for the principal components analysis-multiple linear regression (PCA-MLR) analysis; the detailed method is shown in Hu et al. (2018).

2.4. Darwin model and isoprene sea-air flux calculation

A biogeochemistry and ecosystem model (DARWIN project: http://darwinproject.mit.edu/) was used in this study to model the biomass and community structure of phytoplankton in seawater (Dutkiewicz et al., 2009, 2012). The model was used to understand the diversity and biogeography of the plankton communities in the ocean and is often applied to describe the biochemical activity of the ocean (Wu et al., 2020; Zhang et al., 2020). The model simulated the biogeochemical cycling of phosphorus, nitrogen, carbon, silicon, and iron, and six phytoplankton groups were modelled according to resource competition theory, namely, diatoms, *Synechococcus*, *Prochlorococcus*, *Trichodesmium*, *Coccolithophores* and other large eukaryotes (Dutkiewicz et al., 2015; Losa et al., 2019). Diatoms were found to be an important prolific species in the Southern Ocean (Yassaa et al., 2008). *Prochlorococcus* dominate in the tropical and subtropical oceans with a strong isoprene emission rate (9.66 μmol g[chlorophyll *a*]$^{-1}$ day^{-1}) (Arnold et al., 2009; Shaw et al., 2003). *Synechococcus* and *Trichodesmium* have strong emission rates of isoprene (3–4.97 μmol g[chlorophyll *a*]$^{-1}$ day^{-1}) (Bonsang et al., 2010; Shaw et al., 2003), and *Synechococcus* and *Trichodesmium* mainly exist in the equatorial Pacific and tropical or subtropical regions, respectively (Alvain et al., 2008; Yassaa et al., 2008). A coarse spatial resolution (1° × 1° horizontally) and hourly temporal resolution were used in the simulation.

According to the phytoplankton concentration given by the DARWIN model and the production rate of each phytoplankton (Arnold et al., 2009; Bonsang et al., 2010), isoprene sea-air flux was calculated as shown in Supplementary (Rodríguez-Ros et al., 2020b).

3. Results and discussion

3.1. Spatial distribution of marine atmospheric isoprene

The spatial distributions of marine atmospheric isoprene are shown in Fig. 1. The concentration of isoprene ranged from not detected (ND) to 452 pptv, with a mean and median value of 48 ± 81 pptv and 25 pptv, respectively, and the result showed a large variability. Table 1 lists some field studies of marine atmospheric isoprene. In different sea areas and seasons, isoprene concentrations are different. The mean concentration of atmospheric isoprene collected over oceans in this study was much lower than that in coastal cities and biogenic air passes from vegetation (Emmerson et al., 2018). Some studies reported that isoprene concentrations in the Arctic were very low (<13.82 pptv) (Hackenberg et al., 2017; Hopkins et al., 2002; Mungall et al., 2017). Approximately 63% of the samples collected in CHINARE2012 did not detected isoprene, especially in the Arctic Ocean. In addition, the mean isoprene concentrations collected in CHINARE2012 (12 pptv) were much lower than those collected in CHINARE2011/2012 and CHINARE2012/2013 (60 pptv), which had the most routes located in the Southern Hemisphere oceans. A negative correlation was found between isoprene and latitude ($r = -0.40$, $p < 0.01$). These results showed that marine atmospheric isoprene in the Southern Hemisphere was higher than that in the Northern Hemisphere. The lower isoprene concentration in the Northern Hemisphere agrees with the modelled annual mean concentration of isoprene, which suggests concentrations in the Southern Hemisphere are higher than those in the Northern Hemisphere due to phytoplankton distribution differences (Luo and Yu, 2010b).

The isoprene concentrations collected in CHINARE2011/2012 and CHINARE2012/2013 were higher than those in the UK-South Atlantic (Hackenberg et al., 2017) and almost on the same level as those in other studies over the Pacific Ocean and Indian Ocean (Bonsang et al., 1992; Colomb et al., 2009; Matsunaga et al., 2002). Some high isoprene concentrations were found in the region near the continent, such as the Australian coastal area, and according to the 2-day air mass BTs, the results showed that these samples were influenced by land air mass (shown in Fig. S4). Previous studies reported that marine atmospheric isoprene in the Tropic Ocean region may be affected by land emissions and cause the concentration of isoprene to often exceed 100 pptv (Shaw et al., 2010; Yokouchi et al., 1999). Atmospheric isoprene in Prydz Bay (PB, 60°S-70°S, 68°E−79°E) showed a high value (Fig. 1). Yassaa et al. (2008) reported higher isoprene concentrations (up to 375 pptv) at a sampling site close to chlorophyll-*a* blooms, and high isoprene SOA

Table 1
Marine atmospheric isoprene at different locations.

Locations	Time	Isoprene(pptv)		Reference
		range	mean	
Arctic	Jul–Sep 1999	<1.9		Hopkins et al. (2002)
	Jul, Aug 2014		1.6	Mungall et al. (2017)
	Mar 2013	<13.82	3.17	Hackenberg et al. (2017)
	Jul, Aug 2013	<1.61	0.19	Hackenberg et al. (2017)
Western North Pacific	May 2001	7.2–110	45	Matsunaga et al. (2002)
Southern Pacific	May, Jun 1987	<2-36		Bonsang et al. (1992)
Eastern Pacific	Oct 2015	0–6		Booge et al. (2016)
Southern Indian Ocean	Mar 1986–May 1987	<10-20		Bonsang et al. (1992)
	Dec 2004	20–340	40	Colomb et al. (2009)
Indian Ocean	Jun–Jul 2014	0–10		Booge et al. (2016)
South-east Australia	Dec 2012–Feb 2013		280	Emmerson et al. (2018)
Near tropical islands and Australia	Dec 1996–Jan 1997	100–286		Yokouchi et al. (1999)
UK-South Atlantic	Oct, Nov 2012	<18.28	1.47	Hackenberg et al. (2017)
	Oct, Nov 2013	<10.24	2.72	Hackenberg et al. (2017)
TSO	Jan–Feb 1997	>100		Yokouchi et al. (1999)
	Dec 1997–Mar 1998	<1–57		Yokouchi et al. (1999)
	Jan 2002	<3		Wingenter et al. (2004)
	Jan–Feb 2002	0.03–0.68		Meskhidze and Nenes (2006)
	Jan–Mar 2007	[a] ND-48		Yassaa et al. (2008)
	Jan–Mar 2007	[b] 60-138		Yassaa et al. (2008)
	Jan–Mar 2007	[c] 32-375		Yassaa et al. (2008)
CHINARE2011/2012	Nov–Dec 2011, Feb–Mar 2012	ND-189	32	This study
CHINARE2012	Jul–Sep 2012	ND-74	12	
CHINARE2012/2013	Nov–Dec 2012, Feb–Mar 2013	ND-452	113	

[a] -Far away before the bloom.
[b] -Distant bloom.
[c] -In situ bloom.

(3.9–95 ng/m^3) was found in PB when phytoplankton blooms occur during summer (Hu et al., 2013), indicating that the high isoprene concentration in this region may be caused by phytoplankton emissions. Satellite data of chlorophyll-*a* show high concentrations of chlorophyll-*a* at the time of sampling (Fig. S5).

3.2. Comparison of isoprene flux from oceanic phytoplankton and observed isoprene in the atmosphere

Previous studies have shown that phytoplankton emissions are an important source of isoprene in the remote ocean (Hu et al., 2013; Tran et al., 2013). The DARWIN model was used to model the phytoplankton species and concentrations of the top 100 m of seawater. The discussion here does not include the samples that are influenced by land air mass to avoid the impact of land emissions. In addition, since most samples in CHINARE2012 did not detect isoprene, samples collected in CHINARE2012 were not discussed.

The concentration of total phytoplankton is also high in latitudes south of the 40°S ocean compared to low latitudes (30°S to 30°N). Diatom was the dominating species in latitudes south of the 40°S ocean, in accord with previous studies (Alvain et al., 2008; Yassaa et al., 2008), while *Prochlorococcus* dominated in the low latitude ocean. The production rate of isoprene varies substantially for different phytoplankton species. For example, the emission rate of *Prochlorococcus* is strong (9.66 μmol g[chlorophyll *a*]$^{-1}$ day^{-1}), while the emission rate of *Coccolithophore* is weak (1 μmol g[chlorophyll *a*]$^{-1}$ day^{-1}) (Bonsang et al., 2010; Luo and Yu, 2010; Yassaa et al., 2008). According to the isoprene production rate of each phytoplankton, as shown in Table S2, the isoprene production rate of phytoplankton was calculated. Although the emission rate of diatoms was not the highest (1.21 and 2.48 μmol g[chlorophyll *a*]$^{-1}$ day^{-1} in the South Ocean and elsewhere, respectively) compared to other phytoplankton species (Arnold et al., 2009), diatom was the dominating isoprene-emitting phytoplankton species in latitudes south of 40°S, with a mean production rate of 0.0044 μmol m^{-3} day^{-1} (shown in Fig. 2). *Second, Synechococcus* showed a smaller isoprene production rate in latitudes south of 40°S (0.0003 μmol m^{-3} day^{-1}). At low latitudes, *Prochlorococcus* was the main isoprene-producing species (0.0012 μmol m^{-3} day^{-1}). The total isoprene production rates were significantly different at different sampling sites (Fig. 2 and Table 2). Generally, the Southern Ocean was higher than at low latitudes, and the mean value of the total production rate at latitudes south of 60°S was 0.0045 μmol m^{-3} day^{-1}, 0.0042 μmol m^{-3} day^{-1} at 60°S to 30°S, and 0.0019 μmol m^{-3} day^{-1} at 30°S to 30°N. This result was different from previous work. Conte et al. (2020) found that the isoprene annual production rate by phytoplankton was high between 10°N and 30°S, then decreased above 60°N and 60°S, and decreased with increasing latitude at high latitudes due to the low temperature. The study time was in summer, and the effect of temperature was not considered in this study, which might cause the differences in the work of Conte et al. (2020).

According to the production rate of phytoplankton, the sea-air exchange flux of isoprene was calculated (Fig. 2) to be from 0 to 0.4 μmol m^{-2} day^{-1}, with a mean value of 0.03 μmol m^{-2} day^{-1}. The spatial distribution trend of isoprene flux was 0.03, 0.06 and 0.008 μmol m^{-2} day^{-1} in latitudes south of 60°S, 60°S to 30°S, and 30°S to 30°N, respectively, and showed a different trend to the isoprene production rate. The highest isoprene flux was observed at latitudes between 60 and 30°S, although the production rate was at approximately the same level as those from latitudes south of 60°S. This might be caused by the high wind speed, which may promote the sea-air flux from 60°S to 30°S (11.5 m/s, Table 2). No correlations were found between the flux and observed atmospheric isoprene concentration. A simple box model was used to estimate the atmospheric isoprene concentration according to the emissions flux from the DARWIN model estimate, and the method was referenced in (Booge et al., 2016). Assuming that the atmospheric boundary layer height is 800 m, the atmospheric residence time of isoprene is 1–4 h, and the calculated atmospheric concentration of isoprene is 0.04–0.15 pptv, 300–1400 times lower than that observed. Conte et al. (2020) reported that the oceanic isoprene flux was 0–0.12 μmol m^{-2} day^{-1}, approximately 0.27 Tg C yr^{-1} when considering the biochemical sink; without the biochemical sink, the global oceanic isoprene flux to the atmosphere was 0.32 Tg C yr^{-1} (Luo and Yu, 2010) and 0.27 Tg C yr^{-1} (Arnold et al., 2009). According to the model results, the estimated global oceanic isoprene flux to the atmosphere was 0.22 Tg C yr^{-1} in this study, almost at the same level as previous studies. This means that none of the previous methods based on model calculations can well explain the concentration of isoprene in the atmosphere, and there may be an undiscovered isoprene source. This result is consistent with previous reports (Booge et al., 2016). In addition, other factors in the atmosphere, such as the atmospheric oxidation capacity and wind speed, may also affect isoprene concentrations.

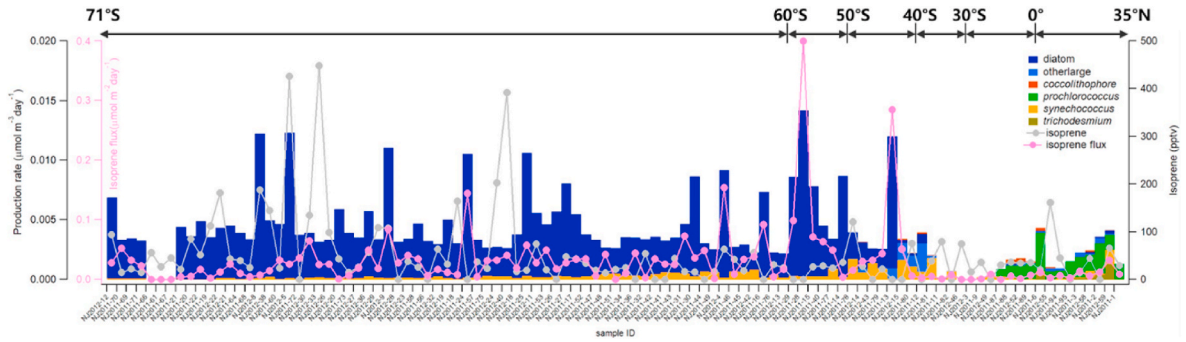

Fig. 2. Observed atmospheric isoprene concentration (right axis), production rate of different phytoplankton species (left axis, black) and the sea-air exchange flux of isoprene (left axis, pink) with different samples. (For interpretation of the references to colour in this figure legend, the reader is referred to the Web version of this article.)

Table 2
The mean isoprene production rate, sea-air exchange flux, and wind speed in different regions.

latitude	production rate (μmol m^{-3} day^{-1})	Flux of isoprene (μmol m^{-2} day^{-1})	Wind speed (m/s)
south of 60°S	0.0045	0.03	9.3
60°S - 30°S	0.0042	0.06	11.5
30°S - 30°N	0.0019	0.008	6.7

3.3. Role of atmospheric removal capacity in marine atmospheric isoprene distribution

Through the comparative discussion in section 3.2, the distributions of atmospheric isoprene and sea-air flux were different. To further discuss the potential influencing factors of marine atmospheric isoprene distribution, PCA-MLR was used to analyse temperature, WS, SST, salinity, HCHO, the concentration and isoprene production rate of phytoplankton, and the isoprene sea-air flux of CHINARE2011/2012 and CHINARE2012/2013 performed by SPSS 20. Table 3 shows the loadings of various environmental variables in the PCA results. Factor 1, Factor 2 and Factor 3 explained 37.11%, 31.29% and 19.38% of the total variance, respectively. Factor 1 had a high loading on temperature, SST, salinity and HCHO. Factor 2 characterized a high loading on phytoplankton concentration, production rate, and the sea-air flux of isoprene. Factor 3 characterized a high loading on WS.

SST and salinity can influence phytoplankton distribution and productivity (Shaw et al., 2003; Sugie et al., 2020). A previous study reported that the isoprene production rate increased with increasing SST when the temperature was higher than 23 °C (Shaw et al., 2003). In addition, high SST has been suggested to promote sea-air exchange (Liss and Merlivat, 1986), thus elevating atmospheric isoprene concentrations. Salinity influences isoprene production (Booge et al., 2018).

Table 3
Loadings of variables in factor analysis by the maximum variance rotation method.

variables	Factor 1	Factor 2	Factor 3
WS	−0.168	0.041	**0.938**
Temperature	**0.897**	−0.278	−0.166
SST	**0.883**	−0.333	−0.183
Salinity	**0.723**	−0.427	0.127
HCHO	**0.797**	−0.018	−0.390
Phytoplankton concentration	−0.333	**0.912**	0.075
Production rate of phytoplankton	−0.231	**0.949**	0.103
Flux	−0.186	**0.631**	**0.651**
% of variance	37.11%	31.29%	19.38%
Cumulative %	37.11%	68.40%	87.78%

Atmospheric isoprene can rapidly react with hydroxyl radicals (OH), and HCHO is an important oxidation component of the isoprene photochemical process and is often used to trace atmospheric isoprene (Marais et al., 2014; Wennberg et al., 2018). Wind speeds can cause isoprene to diffuse and reduce its concentration in the atmosphere. Factor 1 and Factor 3 were considered physical and chemical environmental variables. Factor 2 was considered the marine emission capacity, including isoprene sea-air flux, concentration and production of phytoplankton. Combined with MLR analysis, Factor 1 and Factor 3 contributed 43.63% to atmospheric isoprene, while Factor 2 contributed 56.37% to atmospheric isoprene. This means that at large spatial scales, both emissions and physical and chemical environmental parameters are important for atmospheric isoprene distribution.

For further discussion, samples were divided into two groups (south of 60°S, north of 60°S) to perform PCR-MLR analysis to discuss the geographical difference. Table S3 shows the loadings of various environmental variables of the PCA results at different latitudes. Factor 1, with high loadings of sea-air flux, concentration and production rate of phytoplankton, was considered marine emission capacity. Factor 2, with high loadings of HCHO and wind speed, was considered the atmospheric isoprene removal capacity. Factor 3 contributed by high loadings on air temperature and SST. For the northern region of 60°S, Factor 1 was considered the atmospheric removal capacity and temperature because it showed high loadings on wind speed, temperature, SST and HCHO. Factor 2 has a high loading on the salinity, sea-air flux, concentration and production rate of phytoplankton, considered to be the marine emission capacity.

Fig. 3 shows the relative contributions of different factors at different latitudes. The main controlling factors were different with latitude

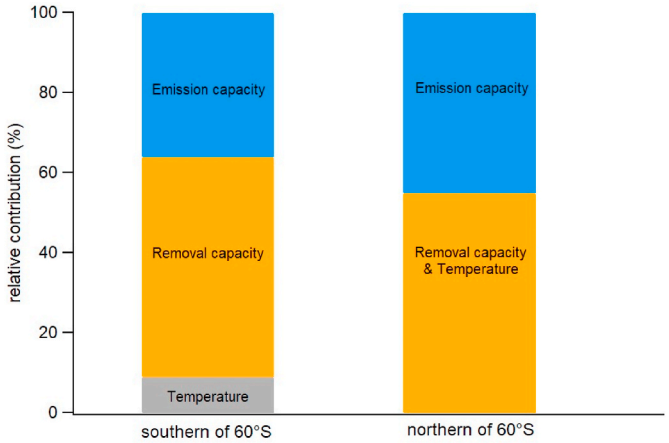

Fig. 3. Relative contribution to marine atmospheric isoprene at different latitudes.

distribution. At latitudes south of 60°S, the atmospheric removal capacity and marine emission capacity contributed 55.05% and 35.98%, respectively. Because the SST (0.85 °C) was low in the Southern Ocean and may limit isoprene production (Rodríguez-Ros et al., 2020a, 2020b), temperature becomes a limiting factor of isoprene production and contributed 8.97%. The relatively low atmospheric oxidation capacity and wind speed result in isoprene accumulation in this region. In latitudes north of 60°S, the marine emission capacity contributed 45.06%. The potential marine emission capacity was relatively important in the northern 60°S, which might be caused by the low concentration and production rate of phytoplankton in the region. Salinity was an important factor affecting isoprene productivity. The atmospheric removal capacity and temperature cannot be completely separated and contribute 54.94%. The atmospheric oxidation capacity in middle and low latitudes is more susceptible to anthropogenic emissions (Ding et al., 2011; Li et al., 2008, 2018), and atmospheric oxidizing ability has always been relatively strong, so the source will be more important.

From the PCA-MLR results at different latitudes, the main controlling factors affecting the atmosphere are different. The atmospheric removal capacity was important for marine atmospheric isoprene distribution, contributing 55.05% to latitudes north of 60°S. Due to the low atmospheric oxidation (Bahm and Khalil, 2004) in the Southern Ocean, high atmospheric isoprene accumulates in the Southern Ocean. At low latitudes, the marine emission capacity was more important.

4. Conclusions

Atmospheric isoprene was measured from the Arctic Ocean to the Southern Ocean in three campaigns. The levels of isoprene ranged from ND to 452 pptv, with an average value of 48 ± 81 pptv, and the results showed a large variability. Atmospheric isoprene has a much lower concentration in the Arctic Ocean than in the Southern Ocean, and a high isoprene value was found in the southern Ocean. A negative correlation was found between isoprene and latitude ($r = -0.40$, $p < 0.01$). The observed atmospheric isoprene was much higher than the modelled estimation, and the spatial distribution of atmospheric isoprene was different from the sea-air flux of marine isoprene in the Southern Hemisphere. The influences of marine atmospheric isoprene are complicated; except for emission sources, environmental variables such as temperature, WS, SST, salinity and atmospheric oxidation can also influence the distribution of isoprene. At large spatial scales, both marine emissions capacity and physical and chemical environmental parameters are important for atmospheric isoprene distribution, contributing 56.37% and 43.63%, respectively, to atmospheric isoprene. At latitudes south of 60°S, atmospheric removal capacity was the most important factor for atmospheric isoprene, contributing 55.05%. In latitudes north of 60°S, the marine emission capacity was more important and contributed 54.94%.

In this study, the photochemical emissions by the microsurface layer and the consumption of isoprene, such as biodegradation and photochemical processes, in seawater were not considered, and more detailed measurements in the air and water phases are needed in the future to explain the influence of environmental variables on marine atmospheric isoprene to better understand the contributions of marine isoprene to SOA in the remote ocean.

CRediT authorship contribution statement

Xiawei Yu: Formal analysis, Writing – original draft, Writing – review & editing, Visualization. **Yanli Zhang:** Formal analysis, Methodology. **Ruilin Jin:** Writing – review & editing. **Zhangyan Chai:** Writing – review & editing. **Qihou Hu:** Investigation. **Juan Yu:** Investigation. **Jie Xing:** Investigation. **Lulu Zhang:** Investigation. **Hui Kang:** Investigation, Resources. **Yanxu Zhang:** Methodology, Writing – review & editing. **Xinming Wang:** Methodology, Writing – review & editing. **Zhouqing Xie:** Conceptualization, Methodology, Writing – review & editing, Supervision, Funding acquisition, Project administration.

Declaration of competing interest

The authors declare that they have no known competing financial interests or personal relationships that could have appeared to influence the work reported in this paper.

Data availability

The data for this paper will be freely available from corresponding author

Acknowledgements and Data

This research was supported by grants from the National Natural Science Foundation of China, China (Project Nos. 41676173, 41941014, 42106219). The Fundamental Research Funds for the Central Universities, China (Project No. WK2080000121) and open fund of Key Lab of Environmental Optics and Technology of Chinese Academy of Sciences, China (Project No. 2005DP173065-2018-02). We thank the Chinese Arctic and Antarctic Administration for logistical support with field campaigns.

The data for this paper will be freely available from Zhouqing Xie. (zqxie@ustc.edu.cn)

Appendix A. Supplementary data

Supplementary data to this article can be found online at https://doi.org/10.1016/j.atmosenv.2022.119414.

References

Alvain, S., Moulin, C., Dandonneau, Y., Loisel, H., 2008. Seasonal distribution and succession of dominant phytoplankton groups in the global ocean: a satellite view. Global Biogeochem. Cycles 22.

Arnold, S., Spracklen, D., Williams, J., Yassaa, N., Sciare, J., Bonsang, B., Gros, V., Peeken, I., Lewis, A., Alvain, S., 2009. Evaluation of the global oceanic isoprene source and its impacts on marine organic carbon aerosol. Atmos. Chem. Phys. 9, 1253–1262.

Böge, O., Miao, Y., Plewka, A., Herrmann, H., 2006. Formation of secondary organic particle phase compounds from isoprene gas-phase oxidation products: an aerosol chamber and field study. Atmos. Environ. 40, 2501–2509.

Bahm, K., Khalil, M.A.K., 2004. A new model of tropospheric hydroxyl radical concentrations. Chemosphere 54, 143–166.

Bates, K.H., Jacob, D.J., 2019. A new model mechanism for atmospheric oxidation of isoprene: global effects on oxidants, nitrogen oxides, organic products, and secondary organic aerosol. Atmos. Chem. Phys. 19, 9613–9640.

Blake, D.R., Smith Jr., T.W., Chen, T.-Y., Whipple, W.J., Rowland, F.S., 1994. Effects of biomass burning on summertime nonmethane hydrocarbon concentrations in the Canadian wetlands. J. Geophys. Res. Atmos. 99, 1699–1719.

Bonsang, B., Gros, V., Peeken, I., Yassaa, N., Bluhm, K., Zöllner, E., Sarda-Esteve, R., Williams, J., 2010. Isoprene emission from phytoplankton monocultures: the relationship with chlorophyll-a, cell volume and carbon content. Environ. Chem. 7, 554–563.

Bonsang, B., Polle, C., Lambert, G., 1992. Evidence for marine production of isoprene. Geophys. Res. Lett. 19, 1129–1132.

Booge, D., Marandino, C.A., Schlundt, C., Palmer, P.I., Schlundt, M., Atlas, E.L., Bracher, A., Saltzman, E.S., Wallace, D.W.R., 2016. Can simple models predict large-scale surface ocean isoprene concentrations? Atmos. Chem. Phys. 16, 11807–11821.

Booge, D., Schlundt, C., Bracher, A., Endres, S., Zäncker, B., Marandino, C.A., 2018. Marine isoprene production and consumption in the mixed layer of the surface ocean – a field study over two oceanic regions. Biogeosciences 15, 649–667.

Brüggemann, M., Hayeck, N., Bonnineau, C., Pesce, S., Alpert, P.A., Perrier, S., Zuth, C., Hoffmann, T., Chen, J., George, C., 2017. Interfacial photochemistry of biogenic surfactants: a major source of abiotic volatile organic compounds. Faraday Discuss 200, 59–74.

Brüggemann, M., Hayeck, N., George, C., 2018. Interfacial photochemistry at the ocean surface is a global source of organic vapors and aerosols. Nat. Commun. 9, 2101.

Ciuraru, R., Fine, L., Pinxteren, M.v., D'Anna, B., Herrmann, H., George, C., 2015. Unravelling new processes at interfaces: photochemical isoprene production at the sea surface. Environ. Sci. Technol. 49, 13199–13205.

Claeys, M., Graham, B., Vas, G., Wang, W., Vermeylen, R., Pashynska, V., Cafmeyer, J., Guyon, P., Andreae, M.O., Artaxo, P., 2004. Formation of secondary organic aerosols through photooxidation of isoprene. Science 303, 1173–1176.

Colomb, A., Gros, V., Alvain, S., Sarda-Esteve, R., Bonsang, B., Moulin, C., Klüpfel, T., Williams, J., 2009. Variation of atmospheric volatile organic compounds over the Southern Indian Ocean (30–49 S). Environ. Chem. 6, 70–82.
Conte, L., Szopa, S., Aumont, O., Gros, V., Bopp, L., 2020. Sources and sinks of isoprene in the global open ocean: simulated patterns and emissions to the atmosphere. J. Geophys. Res.: Oceans 125, e2019JC015946.
Ding, X., Wang, X.-M., Zheng, M., 2011. The influence of temperature and aerosol acidity on biogenic secondary organic aerosol tracers: observations at a rural site in the central Pearl River Delta region, South China. Atmos. Environ. 45, 1303–1311.
Dutkiewicz, S., Follows, M.J., Bragg, J.G., 2009. Modeling the coupling of ocean ecology and biogeochemistry. Global Biogeochem. Cycles 23.
Dutkiewicz, S., Hickman, A.E., Jahn, O., Gregg, W.W., Mouw, C.B., Follows, M.J., 2015. Capturing optically important constituents and properties in a marine biogeochemical and ecosystem model. Biogeosciences 12, 4447–4481.
Dutkiewicz, S., Ward, B.A., Monteiro, F., Follows, M.J., 2012. Interconnection of nitrogen fixers and iron in the Pacific Ocean: theory and numerical simulations. Global Biogeochem. Cycles 26.
Emmerson, K.M., Cope, M.E., Galbally, I.E., Lee, S., Nelson, P.F., 2018. Isoprene and monoterpene emissions in south-east Australia: comparison of a multi-layer canopy model with MEGAN and with atmospheric observations. Atmos. Chem. Phys. 18, 7539–7556.
Fu, D., Millet, D.B., Wells, K.C., Payne, V.H., Yu, S., Guenther, A., Eldering, A., 2019. Direct retrieval of isoprene from satellite-based infrared measurements. Nat. Commun. 10, 3811.
Guenther, A., Karl, T., Harley, P., Wiedinmyer, C., Palmer, P., Geron, C., 2006. Estimates of global terrestrial isoprene emissions using MEGAN (model of emissions of gases and aerosols from nature). Atmos. Chem. Phys. 6.
Hackenberg, S.C., Andrews, S.J., Airs, R., Arnold, S.R., Bouman, H.A., Brewin, R.J.W., Chance, R.J., Cummings, D., Dall'Olmo, G., Lewis, A.C., Minaeian, J.K., Reifel, K.M., Small, A., Tarran, G.A., Tilstone, G.H., Carpenter, L.J., 2017. Potential controls of isoprene in the surface ocean. Global Biogeochem. Cycles 31, 644–662.
He, P., Bian, L., Zheng, X., Yu, J., Sun, C., Ye, P., Xie, Z., 2016. Observation of surface ozone in the marine boundary layer along a cruise through the Arctic Ocean: from offshore to remote. Atmos. Res. 169, 191–198.
Hopkins, J., Jones, I., Lewis, A., McQuaid, J., Seakins, P., 2002. Non-methane hydrocarbons in the Arctic boundary layer. Atmos. Environ. 36, 3217–3229.
Hu, Q.-H., Xie, Z.-Q., Wang, X.-M., Kang, H., He, Q.-F., Zhang, P., 2013. Secondary organic aerosols over oceans via oxidation of isoprene and monoterpenes from Arctic to Antarctic. Sci. Rep. 3.
Hu, Q., Xie, Z., Wang, X., Kang, H., Zhang, Y., Ding, X., Zhang, P., 2018. Monocarboxylic and dicarboxylic acids over oceans from the East China Sea to the Arctic Ocean: roles of ocean emissions, continental input and secondary formation. Sci. Total Environ. 640–641, 284–292.
Hu, Q., Xie, Z., Wang, X., Yu, J., Zhang, Y., 2016. Methyl iodine over oceans from the Arctic Ocean to the maritime antarctic. Sci. Rep. 6, 26007.
IPCC, 2018. In: Masson-Delmotte, V., P.Z., Pörtner, H.-O., Roberts, D., Skea, J., Shukla, P. R., Pirani, A., Moufouma-Okia, W., Péan, C., Pidcock, R., Connors, S., Matthews, J.B. R., Chen, Y., Zhou, X., Gomis, M.I., Lonnoy, E., Maycock, T., Tignor, M., T.W. (Eds.), Global Warming of 1.5°C. An IPCC Special Report on the Impacts of Global Warming of 1.5°C above Pre-industrial Levels and Related Global Greenhouse Gas Emission Pathways, in the Context of Strengthening the Global Response to the Threat of Climate Change, Sustainable Development, and Efforts to Eradicate Poverty.
IPCC, 2019. In: Pörtner, H.-O., Roberts, D.C., Masson-Delmotte, V., Zhai, P., M.T., Poloczanska, E., Mintenbeck, K., Alegría, A., Nicolai, M., Okem, A., Petzold, J., Rama, B., N.M.W. (Eds.), IPCC Special Report on the Ocean and Cryosphere in a Changing Climate.
Lewis, A.C., Carpenter, L.J., Pilling, M.J., 2001. Nonmethane hydrocarbons in Southern Ocean boundary layer air. J. Geophys. Res. Atmos. 106, 4987–4994.
Li, J., Wang, G., Wu, C., Cao, C., Ren, Y., Wang, J., Li, J., Cao, J., Zeng, L., Zhu, T., 2018. Characterization of isoprene-derived secondary organic aerosols at a rural site in North China Plain with implications for anthropogenic pollution effects. Sci. Rep. 8, 535.
Li, S., Matthews, J., Sinha, A., 2008. Atmospheric hydroxyl radical production from electronically excited NO2 and H2O. Science 319, 1657–1660.
Liakakou, E., Vrekoussis, M., Bonsang, B., Donousis, C., Kanakidou, M., Mihalopoulos, N., 2007. Isoprene above the Eastern Mediterranean: seasonal variation and contribution to the oxidation capacity of the atmosphere. Atmos. Environ. 41, 1002–1010.
Liss, P., Merlivat, L., 1986. Air-sea gas exchange rates: introduction and synthesis. In: Buat-Ménard, P. (Ed.), The Role of Air-Sea Exchange in Geochemical Cycling. NATO ASI Series 185, pp. 113–127.
Losa, S.N., Dutkiewicz, S., Losch, M., Oelker, J., Soppa, M.A., Trimborn, S., Xi, H., Bracher, A., 2019. On modeling the southern Ocean phytoplankton functional types. Biogeosci. Discuss. 2019, 1–37.
Luo, G., Yu, F., 2010. A numerical evaluation of global oceanic emissions of α-pinene and isoprene. Atmos. Chem. Phys. 10, 2007–2015.
Marais, E.A., Jacob, D.J., Guenther, A., Chance, K., Kurosu, T.P., Murphy, J.G., Reeves, C. E., Pye, H.O.T., 2014. Improved model of isoprene emissions in Africa using Ozone Monitoring Instrument (OMI) satellite observations of formaldehyde: implications for oxidants and particulate matter. Atmos. Chem. Phys. 14, 7693–7703.
Matsunaga, S., Mochida, M., Saito, T., Kawamura, K., 2002. In situ measurement of isoprene in the marine air and surface seawater from the western North Pacific. Atmos. Environ. 36, 6051–6057.
Meskhidze, N., Nenes, A., 2006. Phytoplankton and cloudiness in the southern Ocean. Science 314, 1419–1423.
Mungall, E.L., Abbatt, J.P.D., Wentzell, J.J.B., Lee, A.K.Y., Thomas, J.L., Blais, M., Gosselin, M., Miller, L.A., Papakyriakou, T., Willis, M.D., Liggio, J., 2017. Microlayer source of oxygenated volatile organic compounds in the summertime marine Arctic boundary layer. Proc. Natl. Acad. Sci. USA 114, 6203–6208.
Novak, G.A., Bertram, T.H., 2020. Reactive VOC production from photochemical and heterogeneous reactions occurring at the air–ocean interface. Acc. Chem. Res. 53, 1014–1023.
Palmer, P.I., Shaw, S.L., 2005. Quantifying global marine isoprene fluxes using MODIS chlorophyll observations. Geophys. Res. Lett. 32.
Rodríguez-Ros, P., Cortés, P., Robinson, C.M., Nunes, S., Hassler, C., Royer, S.-J., Estrada, M., Sala, M.M., Simó, R., 2020a. Distribution and drivers of marine isoprene concentration across the southern Ocean. Atmosphere 11, 556.
Rodríguez-Ros, P., Galí, M., Cortés, P., Robinson, C.M., Antoine, D., Wohl, C., Yang, M., Simó, R., 2020b. Remote sensing retrieval of isoprene concentrations in the southern Ocean. Geophys. Res. Lett. 47, e2020GL087888.
Shaw, S.L., Chisholm, S.W., Prinn, R.G., 2003. Isoprene production by Prochlorococcus, a marine cyanobacterium, and other phytoplankton. Mar. Chem. 80, 227–245.
Shaw, S.L., Gantt, B., Meskhidze, N., 2010. Production and emissions of marine isoprene and monoterpenes: a review. Adv. Meteorol. 2010.
Sugie, K., Fujiwara, A., Nishino, S., Kameyama, S., Harada, N., 2020. Impacts of temperature, CO2, and salinity on phytoplankton community composition in the western Arctic Ocean. Front. Mar. Sci. 6.
Tran, S., Bonsang, B., Gros, V., Peeken, I., Sarda-Esteve, R., Bernhardt, A., Belviso, S., 2013. A survey of carbon monoxide and non-methane hydrocarbons in the Arctic Ocean during summer 2010. Biogeosciences 10, 1909–1935.
Wells, K.C., Millet, D.B., Payne, V.H., Deventer, M.J., Bates, K.H., de Gouw, J.A., Graus, M., Warneke, C., Wisthaler, A., Fuentes, J.D., 2020. Satellite isoprene retrievals constrain emissions and atmospheric oxidation. Nature 585, 225–233.
Wennberg, P.O., Bates, K.H., Crounse, J.D., Dodson, L.G., McVay, R.C., Mertens, L.A., Nguyen, T.B., Praske, E., Schwantes, R.H., Smarte, M.D., St Clair, J.M., Teng, A.P., Zhang, X., Seinfeld, J.H., 2018. Gas-phase reactions of isoprene and its major oxidation products. Chem. Rev. 118, 3337–3390.
Wingenter, Oliver W., Haase, Karl B., Strutton, Peter, Friederich, Gernot, Meinardi, Simone, Blake, Donald R., Rowland, F. Sherwood, 2004. Changing concentrations of CO, CH_4, C_5H_8, CH_3Br, CH_3I, and dimethyl sulfide during the Southern Ocean Iron Enrichment Experiments. Proc. Natl. Acad. Sci. U.S.A. 101.
Wu, P., Zakem, E.J., Dutkiewicz, S., Zhang, Y., 2020. Biomagnification of methylmercury in a marine plankton ecosystem. Environ. Sci. Technol. 54, 5446–5455.
Yassaa, N., Peeken, I., Zöllner, E., Bluhm, K., Arnold, S., Spracklen, D., Williams, J., 2008. Evidence for marine production of monoterpenes. Environ. Chem. 5, 391.
Yokouchi, Y., Li, H.J., Machida, T., Aoki, S., Akimoto, H., 1999. Isoprene in the marine boundary layer (southeast asian sea, eastern Indian ocean, and southern Ocean): comparison with dimethyl sulfide and bromoform. J. Geophys. Res. Atmos. 104, 8067–8076.
Zhang, Y., Soerensen, A.L., Schartup, A.T., Sunderland, E.M., 2020. A global model for methylmercury formation and uptake at the base of marine food webs. Global Biogeochem. Cycles 34, e2019GB006348.
Zhang, Y., Wang, X., Blake, D.R., Li, L., Zhang, Z., Wang, S., Guo, H., Lee, F.S., Gao, B., Chan, L., 2012. Aromatic hydrocarbons as ozone precursors before and after outbreak of the 2008 financial crisis in the Pearl River Delta region, south China. J. Geophys. Res. Atmos. 117.